Bioorganic Chemistry 91 (2019) 103141

Contents lists available at ScienceDirect

Bioorganic Chemistry

journal homepage: www.elsevier.com/locate/bioorg

A solid-phase method for synthesis of dimeric and trimeric ligands: Identification of potent bivalent ligands of 14-3-3σ

Yeongju Lee[1], Brian Chung[1], Daseul Ko, Hyun-Suk Lim*

Department of Chemistry and Division of Advanced Material Science, Pohang University of Science and Technology (POSTECH), Pohang 37673, South Korea

A B S T R A C T

Multivalent protein-protein interactions including bivalent and trivalent interactions play a critical role in mediating a wide range of biological processes. Hence, there is a significant interest in developing molecules that can modulate those signaling pathways mediated by multivalent interactions. For example, multimeric molecules capable of binding to a receptor protein through a multivalent interaction could serve as modulators of such interactions. However, it is challenging to efficiently generate such multimeric ligands. Here, we have developed a facile solid-phase method that allows for the rapid generation of (homo- and hetero-) dimeric and trimeric protein ligands. The feasibility of this strategy was demonstrated by efficiently synthesizing fluorescently-labeled dimeric peptide ligands, which led to dramatically increased binding affinities (~400-fold improvement) relative to a monomeric 14-3-3σ protein ligand.

1. Introduction

Many biological processes are mediated by multivalent binding interactions, such as bivalent and trivalent interactions [1,2]. For instance, ligand-induced multimerization of cell surface receptor proteins often plays a critical role in relaying cellular signal transductions, and thus aberrant interactions are implicated in many disease states. As such, there is a great interest in developing synthetic molecules that can modulate those signaling pathways mediated by multivalent interactions [3,4]. These molecules could serve as invaluable research tools to uncover the biological roles of the interactions and furthermore can be developed as therapeutic candidates for the treatment of associated diseases. One approach to generate such molecules is to design multimeric molecules capable of binding to a receptor protein through a multivalent interaction. A great deal of efforts has been devoted to developing dimeric and trimeric ligands targeting various target proteins [2,5–11]. For example, Guichard and Hoebeke reported that synthetic trivalent peptide ligands mimicking CD40L homotrimers were shown to effectively disrupt the interaction between CD40 receptor, member of the tumor necrosis factor receptor family, and its ligand protein CD40L [12]. More recently, Strømgaard and coworkers designed dimeric peptides capable of binding the two neighboring PDZ domains of PSD-95 protein through a bivalent manner, leading to the discovery of high affinity inhibitors [13].

Most multimeric ligands were typically prepared by solution-phase synthesis, which requires time-consuming and laborious purification processes. In contrast, solid-phase methodology is generally far more convenient and efficient in generating such ligands. However, solid-phase methods are rare [14] and have yet to be explored. Here, we report a facile solid-phase method that allows for the rapid generation of dimeric and trimeric protein ligands. We also demonstrate the utility of our method by developing dimeric peptide inhibitors of 14-3-3σ displaying a remarkably enhanced binding affinity (400-fold improvement) compared to a known monomeric peptide ligand.

2. Results and discussion

2.1. Chemistry

Our synthetic strategy for preparing dimeric and trimeric ligands was to utilize 1,3,5-triazine as a core scaffold. Due to its ease of structural manipulation and inexpensive price as a starting material, triazine has been widely used as a chemical library scaffold and frequently found in numerous biologically active molecules [15–23]. Given that 1,3,5-triazine has three substitution sites that can be modified by three different side chains through stepwise nucleophilic substitutions on cyanuric chloride [15,24,25], 1,3,5-triazine can be used for a versatile scaffolding structure for solid-phase synthesis of dimeric and trimeric protein ligands (Fig. 1). It is important to note that this method can also synthesize heteromultivalent ligands, in addition to homomultivalent ligands, by utilizing orthogonal protecting groups at each of three positions.

To prove the feasibility of our strategy, we chose 14-3-3σ as a model system. 14-3-3σ, one member of the seven 14-3-3 protein family, is a

* Corresponding author.
E-mail address: hslim@postech.ac.kr (H.-S. Lim).
[1] These authors contributed equally.

https://doi.org/10.1016/j.bioorg.2019.103141
Received 23 April 2019; Received in revised form 12 July 2019; Accepted 19 July 2019
Available online 26 July 2019

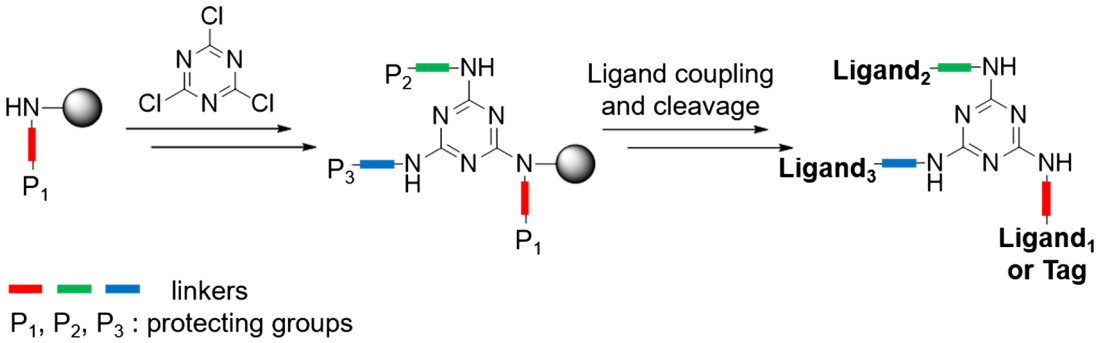

Fig. 1. Solid-phase approach to synthesize dimeric or trimeric peptides.

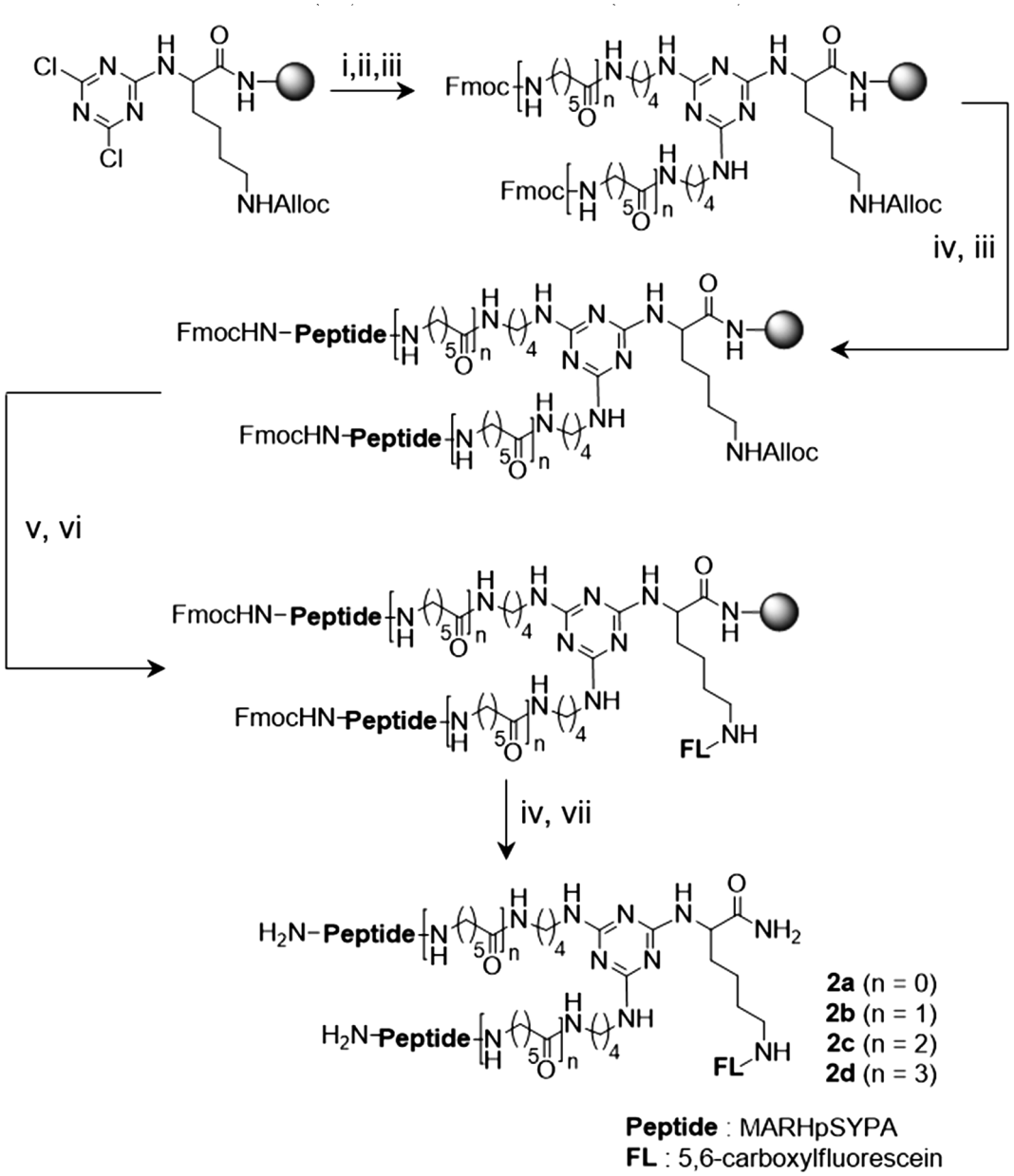

Scheme 1. Solid-phase synthesis of fluorescein labeled dimeric peptides targeting 14-3-3σ. (i) N^1-tritylbutane-1,4-diamine, DIPEA, NMP, 70 °C, 4 h; (ii) TFA/TIPS/DCM (5:5:90), rt, 2 min, 7 times; (iii) HBTU, HOBt, DIPEA, rt, 2 h; (iv) 20% piperidine in DMF, rt, 10 min, 2 times; (v) $Pd(PPh_3)_4$, $PhSiH_3$, dry DCM, rt, 2 h; (vi) DIC, HOBt, 5,6-carboxyfluorescein, DCM: DMF = 1: 1, rt, 4 h; (vii) TFA/TIPS/DCM (95:2.5:2.5), rt, 4 h.

Table 1
Chemical structures and characterization information for monomeric peptide **1** and dimeric peptides **2a-d** with various linker lengths as fluorescently-labeled derivatives.

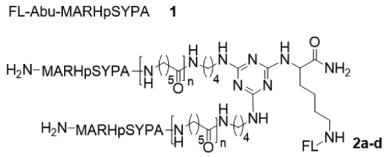

Compd[a]	n	calcd mass $[M + H]^+$	obsd mass $[M + H]^+$	obsd mass $[M + 2H]^{2+}$	obsd mass $[M + 3H]^{3+}$	obsd mass $[M + 4H]^{4+}$	obsd mass $[M + 5H]^{5+}$
1	·	1541.38	1541.4	771.19	N.D.	N.D.	N.D.
2a	0	2916.20	N.D.	1458.60	972.73	729.80	584.04
2b	1	3142.37	N.D.	1571.69	1048.12	786.34	629.27
2c	2	3368.53	N.D.	1684.77	1123.51	842.88	674.51
2d	3	3593.70	N.D.	1797.35	1198.57	899.18	719.54

[a] Compounds were synthesized using L-form amino acids.

multifunctional protein that regulates a wide range of signaling pathways by interacting with a plethora of functionally diverse proteins [26,27]. 14-3-3σ is frequently overexpressed in various human cancers and its dysregulation is linked to cancer progression [26,28]. Hence, 14-3-3σ is emerging as a promising therapeutic target for the treatment of cancers, and the development of molecules capable of inhibiting its function is of significant interest in chemical biology and drug discovery [29–35]. 14-3-3σ recognizes phosphoserine or phosphothreonine-containing motifs of its effector proteins [36]. In addition, dimerization is essential for 14-3-3σ functions, and many effector proteins bind to 14-3-3σ in a bivalent fashion. As a result, bivalent inhibitors of 14-3-3σ recognizing the two identical phosphorylated motifs would have far stronger ability to disrupt the interaction between 14-3-3σ and its effector proteins than monovalent inhibitors [31,35,37,38]. We designed a series of dimeric ligands targeting 14-3-3σ, which also have fluorescence tags for fluorescence polarization (FP)-based binding assays (Scheme 1, Table 1).

For the synthesis of dimeric peptide ligands tagged with a fluorescence dye, Fmoc-L-Lys(Alloc)-OH was first loaded on NH_2-functionalized MBHA resin under standard peptide coupling conditions (Scheme 1). After the removal of Fmoc protecting group, the amine was capped with triazine by treating with cyanuric chloride. The two remaining chlorides on triazine were substituted with N^1-tritylbutane-1,4-diamine in the presence of DIPEA in NMP at 70 °C. After removal of trityl group, different numbers of aminohexanoic acid (Ahx) as linkers were conjugated using standard Fmoc chemistry. Subsequently, eight amino acid residues containing phosphoserine (MARHpSYPA), a known peptide ligand sequence for 14-3-3σ [36], were introduced. Following Alloc deprotection, 5,6-carboxyfluorescein was coupled to the NH_2 in Lys residue. Finally, the resin was treated with 95% trifluoroacetic acid (TFA) for global deprotection and cleavage reaction. The released crude bivalent peptides were characterized by LC/MS and purified by reverse-phase HPLC for further biochemical experiments. Using this solid-phase route, we synthesized four bivalent peptides **2a-d** with different linker length (Table 1).

2.2. Biological evaluation

2.2.1. In vitro binding assay and molecular dynamic (MD) simulations

To evaluate the binding activity of the synthesized fluorescently-labeled bivalent peptides, we employed FP assays. The bivalent or monovalent peptides as fluorescence probes were titrated with varying concentrations of recombinant human 14-3-3σ, and FP was measured (Fig. 2). The binding assay results showed that **2a**, having the shortest linker, exhibited slightly improved 14-3-3σ binding affinity with the K_D value of 12.3 μM, compared to parent monomeric peptide **1**

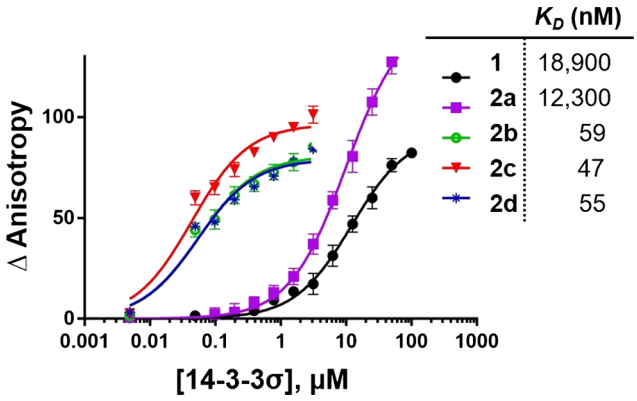

Fig. 2. Binding curves of fluorescein-labeled monomeric and dimeric ligands to 14-3-3σ as determined by a fluorescence polarization-based binding assay. Error bars represent standard deviation from three independent experiments.

(K_D = 18.9 μM). The result indicates that **2a** may bind to 14-3-3σ like a monomer rather than interacting in a bipartite manner due to its short linker length. In contrast, the other dimeric peptides **2b-d** with longer linker length (with 1 to 3 Ahx residues) led to a remarkable ~400-fold enhancement of the 14-3-3σ affinity (K_D = 47–59 nM) compared with monomeric ligand **1** (Fig. 2). Among the synthesized dimeric ligands, **2c** containing two Ahx residues was chosen for further cell-based study.

In order to understand the enhanced binding affinity of dimeric peptides depending on the linker length, we used molecular dynamics (MD) simulations. As illustrated in Fig. 3a, MD simulation of **2c-nf**, an analogue of dimer **2c** displaying the best binding affinity, with the reported crystal structure of 14-3-3σ revealed that two peptide motifs connected by the linker bound to each of dimeric 14-3-3σ, demonstrating that the synthesized dimeric peptide ligands interact with 14-3-3σ in a bivalent manner. In contrast, MD simulation of **2a-nf**, an analogue of dimer **2a** showing the similar binding affinity with the monomeric peptide, showed that only one peptide motif bound to dimeric 14-3-3σ while the other peptide part partially interact with the protein likely due to its relatively short linker length, thereby interacting with 14-3-3σ in a monovalent manner (Fig. 3b). This result suggests that sufficient linker length is essential for a bivalent ligand to make a bidentate interaction with dimeric 14-3-3σ as anticipated.

2.2.2. Cytotoxicity assay

Finally, we explored the cellular activity of dimeric peptide **2c** as a 14-3-3σ inhibitor. 14-3-3σ has been associated with cancer progression by direct interaction with its partner proteins such as p53 tumor suppressor protein. Given its crucial role in tumorigenesis, disruption of the

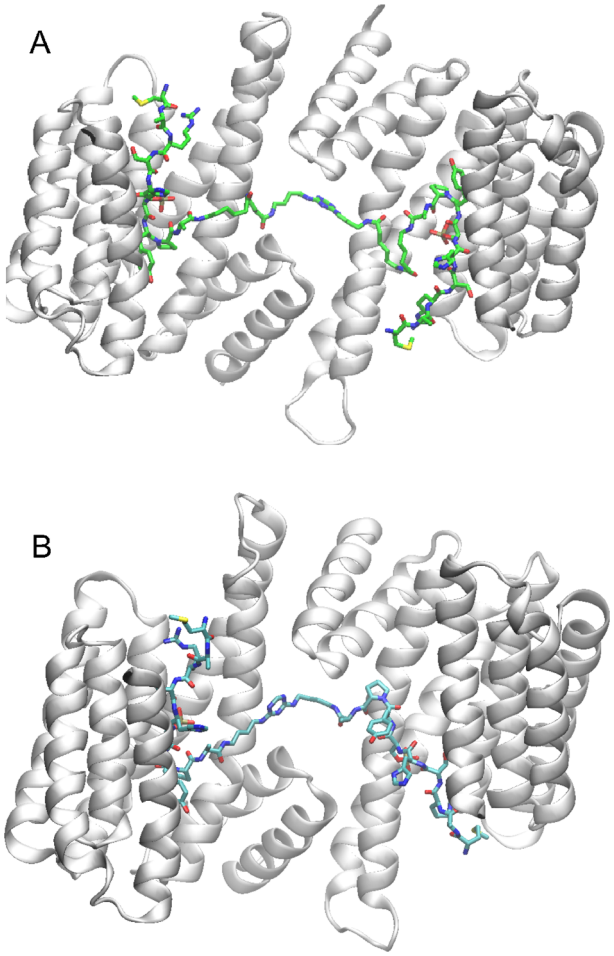

Fig. 3. (A) The predicted binding mode of **2c-nf** (green, **2c** analogue without fluorescein tag) and 14-3-3σ protein (grey) complex by MD simulation. (B) The predicted binding mode of **2a-nf** (blue, **2a** analogue without fluorescein tag) and 14-3-3σ protein (grey) complex by MD simulation.

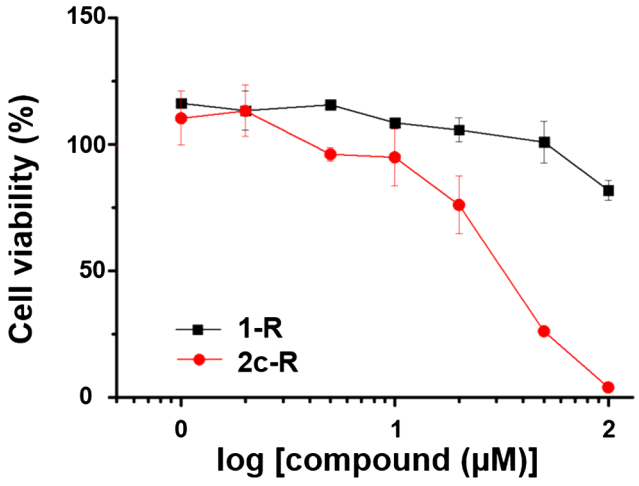

Fig. 4. Dimeric peptide **2c-R** (**2c** analogue containing cell penetrating peptide, Arg_8) efficiently suppresses cancer cell growth whereas monomeric peptide **1-R** (**1** analogue containing Arg_8) had little activity on cell viability. DU145 human prostate cancer cells were treated with **2c-R** or **1-R** for 24 h, and cell viability was assessed by the XTT cell proliferation assay. Error bars represent standard deviation from three independent experiments.

protein-protein interaction between homo-dimeric 14-3-3σ and its interacting partners by **2c** would lead to cell cycle arrest and apoptotic cell death in cancers [30,39]. To test this, dimeric peptide analogue **2c-R** containing a cell-penetrating peptide (Arg_8) was synthesized and treated to DU145 human prostate cancer cells that express 14-3-3σ. The cytotoxicity of **2c-R** and **1-R** (monomeric peptide conjugated with Arg_8) was assessed using the XTT cell proliferation assay (Fig. 4). Not surprisingly, dimeric peptide **2c-R** considerably suppressed prostate cancer cell growth in a dose-dependent manner while monomeric peptide **1-R** had little cell toxicity, highlighting that the dimeric bivalent peptide ligand is indeed far more effective in inhibiting the 14-3-3σ interactions with its partners than the monovalent peptide.

3. Conclusion

In summary, we have developed a facile solid-phase synthetic method that allows for rapid generation of dimeric and trimeric protein ligands by on-resin stepwise substitution reactions on 1,3,5-triazine. Notably, our strategy enables to prepare not only homomultivalent ligands but also heteromultivalent ligands by employing appropriate protecting groups at each of three positions of the 1,3,5-triazine scaffold. We successfully demonstrated the applicability of our method by efficiently synthesizing a series of fluorescently-labeled dimeric peptide ligands (as a result, being trivalent ligands) targeting 14-3-3σ. We have found that such dimeric peptides indeed exhibited markedly enhanced binding affinity (~400-fold improvement) to 14-3-3σ and cellular activity, in comparison with a monomeric peptide ligand. We believe that our solid-phase strategy is highly versatile and can be readily applied to prepare (both homo- and hetero-) multivalent ligands of any protein targets involved in multimeric interactions.

4. Experimental section

4.1. Chemistry

General: All chemicals and reagents were purchased from Sigma-Aldrich, Alfa Aesar, Novabiochem, and TCI. Purchased reagents were directly used without further purification. Fluorenylmethyloxycarbonyl (Fmoc)-protected amino acids and rink amide MBHA resins (0.75 mmol/g) were purchased from Novabiochem. The LC/MS characterization for synthesized peptides was performed on an Agilent 1200 LC/MS system (Agilent Technology) with a C18 reverse phase HPLC column (Eclipse XDB, 3.5 μm, 4.6 mm × 150 mm). A gradient elution of 10% B to 100% B in 7 min was used at flow rate of 0.7 mL/min (solvent A: 100% H_2O, 0.1% trifluoroacetic acid (TFA); B: 100% acetonitrile, 0.1%TFA). The preparative HPLC purification for the crude peptides was performed on an Agilent 1120 Compact LC system (Agilent Technology) with a C18 reversed phase column (Eclipse XDB, 5 μm, 21.2 mm × 150 mm) with a linear gradient from 10% B to 100% B by changing solvent composition over 40 min. High resolution ESI mass spectrometer analysis was performed on the Synapt G2-HDMS mass spectrometer (Waters, Manchester, U.K.), which was operated on the MassLynx 4.1 software.

4.1.1. Synthesis of fluorescein-labeled 9-residue linear phosphopeptide *1* (MARSHpSYPA)

Rink amide MBHA resins (100 mg, 75 μmol) were loaded in a 5 mL fritted syringe and swollen in DMF for 2 h at room temperature (rt). The Fmoc protection group was deprotected by treating with 20% piperidine in DMF (2 × 10 min). The beads were treated with Fmoc protected amino acid (5 equiv.) in the presence of HBTU (5 equiv.), HOBt (5 equiv.), and DIPEA (10 equiv.) in DMF (1 mL) at rt for 2 h. After peptide coupling reaction, the reaction mixture was drained, and the resins were washed with DMF (3×), MeOH (3×), CH_2Cl_2 (3×), and DMF (3×). This process was repeated to afford the desired 9-residue peptide. To the *N*-terminal amine of the resulting peptide,

aminohexanoic acid (Ahx) residue was introduced as a spacer. After removal of Fmoc protecting group, 5,6-carboxyfluorescein was coupled under the same peptide coupling procedure. The synthesized peptide was then cleaved from the resin by treating with 1 mL of a cleavage cocktail (92.5% TFA, 2.5% triisopropylsilane (TIPS), 2.5% thioanisole, and 2.5% D.W) for 2 h. The crude product was then purified by reverse-phase HPLC.

4.1.2. Synthesis of fluorescein-labeled bivalent phosphopeptides (**2a-2d**)

The Fmoc protecting group was removed from the swollen resin as previously described. Next, Fmoc-Lys(Alloc)-OH was subsequently coupled to the resin under the standard peptide coupling condition. After the removal of Fmoc protecting group, the *N*-terminus of the peptide was coupled with triazine by treating cyanuric chloride (5 equiv.) and DIPEA (6 equiv.) in THF at rt for 3 h. The two remaining chlorides on the triazine were substituted with *N*-tritylbutane-1,4-diamine (10 equiv.) and DIPEA (10 equiv.) in NMP at 70 °C for 4 h. The Trt protecting group was removed by treating with 5% TFA and 5% TIPS in CH_2Cl_2 (10 × 2 min). After the beads were neutralized by incubating with 10% DIPEA in DMF for 1 h, Fmoc-Ahx-OH coupling was performed when needed, and this process was repeated from 0 to 3 times depending on the linker length. Then Fmoc protecting group was removed, and peptide coupling was repeated to acquire the desired bivalent phosphopeptides. Alloc protecting group was eliminated by treating with $Pd(PPh_3)_4$ (0.2 equiv.) and $PhSiH_3$ (10 equiv.) in anhydrous CH_2Cl_2 for 2 h at rt. Next, 5,6-carboxyfluorescein (5 equiv.) was coupled to the *N*-terminus using the same peptide coupling procedure.

4.1.3. Synthesis of a N_3 coupled 8-residue poly arginine (N_3-Arg_8)

Following the removal of Fmoc protecting group from the swollen resin, Fmoc-Lys(N_3)-OH was introduced to the resins under the standard peptide coupling conditions. After the Fmoc protecting group was removed, Fmoc-Arg(Pbf)-OH was coupled to obtain 8-mer poly-arginine. The synthesized peptide was cleaved from the resins by treating with 1 mL of a cleavage cocktail for 5 h at rt. The crude product was purified by HPLC.

4.1.4. Synthesis of a cell penetrating monovalent phosphopeptides (**1-R**)

After the Fmoc protecting group from the swollen resin was removed, Fmoc-propargyl-Gly-OH was coupled under the standard peptide coupling condition. After the Fmoc protecting group was removed again, the desiring peptide sequence (MARSHpSYPA) were coupled as described on Section 4.1.1. The peptide was cleaved from the resin by treating with the cleavage cocktail for 2 h. The crude product was purified by HPLC. Then 2 μM of the purified 9-mer peptide was coupled to 2 μM of the prepared cell penetrating peptide, Arg_8, using the Cu(I)-catalyzed click chemistry by treating $CuSO_4{\cdot}5H_2O$ (1 equiv.) and sodium ascorbate (4 equiv.) in 100 μL of H_2O : tBuOH = 1 : 1 solution at rt for 12 h. After the reaction completion was confirmed by LC-MS, the crude product was purified HPLC.

4.1.5. Synthesis of a cell penetrating bivalent phosphopeptide (**2c-R**)

After treating 20% piperidine to swollen resin to remove the Fmoc protecting group, Fmoc-propargyl-Gly-OH was coupled under the same peptide coupling conditions. After deprotection of the Fmoc group, cyanuric chloride and *N*-trityl butane-1,4-diamine linkers were conjugated as described in Section 4.1.2. The Trt protecting group was then removed by treating with 5% TFA and 5% TIPS in CH_2Cl_2 (10 × 2 min). After neutralization with 10% DIPEA in DMF for 1 h at rt, Fmoc-Ahx-OH was added twice under the conventional peptide coupling conditions. After the Fmoc group was deprotected, the peptide coupling procedure was done as described in Section 4.1.1. The crude product cleaved from the resins by the cleavage cocktail were subjected to HPLC purification. Finally, the purified bivalent phosphopeptide was coupled to the azide-containing Arg_8 cell-penetrating peptide via Click chemistry as described in Section 4.1.4.

4.2. Biological evaluation

4.2.1. Expression and purification

GST-tagged fusion 14-3-3σ protein was expressed in an E. coli. BL21 strain purchased from Sigma Aldrich. 14-3-3σ protein purification was performed as described previously [40].

4.2.2. Fluorescence polarization (FP) assay

10 nM of each of the fluorescein-labeled monomeric and dimeric peptides (**1** and **2a-d**) was incubated with varying concentrations of 14-3-3σ protein in binding buffer (50 mM HEPES, pH 7.4, 1 mM EDTA, 150 mM NaCl, and 0.05%Tween-20) in a black Costar 384-well plate for 30 min. The fluorescence anisotropy was measured on a Tecan F200 Microplate Reader (λ_{Ex}: 485 nm; λ_{Em}: 535 nm). The dissociation constant of the protein-ligand complex (K_D) was determined by GraphPad Prism® 4 (San Diego, CA) software with non-linear regression and fitted using following equation, $Y = B_{max} \times X/(K_D + X)$.

4.2.3. Cell culture

DU145 cells were maintained in Dulbecco's modified Eagle medium (DMEM) containing 10% fetal bovine serum (FBS), and penicillin-streptomycin with 5% CO_2 at 37 °C.

4.2.4. Cytotoxicity assay

1×10^4 DU145 human prostate cancer cells were seeded in a 96-well plate for 24 h. Cells were treated with varying concentrations of **2c-R**, **1-R**, or DMSO for 24 h in Opti-MEM medium. Cell viability was measured by Cyto X Cell Viability Assay kit (LPS solution) according to the manufacturer's instruction.

4.3. Molecular dynamics (MD) simulations

The inputs for the computational experiments were prepared using Quick MD simulator on the CHARMM-GUI web site. The initial structure of **2a-nf** or **2c-nf** was built from the reported crystal structure of 14-3-3σ in complex with a phosphopeptide (PDB ID: 1YWT) using Quick MD Simulator and CHRAMM General Force Field [41]. **2a-nf** or **2c-nf** was subjected to energy-minimization with the CHRAMM General Force Field (c41b1). Energy-minimized **2a-nf** or **2c-nf** structure was solvated with TIP3P water in a periodic truncated rectangular box that the box sizes were set to 110 Å in X, Y, and Z. and the neutralization of the system with sodium and chloride ions was followed. MD simulation was carried out by NAMD inputs (v2.12). A total of three independent explicit-solvent MD simulations using different initial atomic velocities were carried out. The system has undergone equilibration run and the production (100 ns) run, which were carried out at 298.15 K and 1 atm.

Declaration of Competing Interest

Author declares that there is no conflicts of interest.

Acknowledgments

This work was supported by the National Research Foundation of Korea (NRF) grant funded by the Korea government (MSIT) (NRF-2017R1A2B3004941 and NRF-2018R1A4A1024713).

Appendix A. Supplementary material

Supplementary data to this article can be found online at https://doi.org/10.1016/j.bioorg.2019.103141.

References

[1] M. Mammen, S.-K. Choi, G.M. Whitesides, Angew. Chem. Int. Ed. 37 (1998) 2754–2794.

[2] A. Whitty, C.W. Borysenko, Chem. Biol. 6 (1999) 107–118.
[3] L.L. Kiessling, J.E. Gestwicki, L.E. Strong, Curr. Opin. Chem. Biol. 4 (2000) 696–703.
[4] L.L. Kiessling, J.E. Gestwicki, L.E. Strong, Angew. Chem. Int. Ed. 45 (2006) 2348–2368.
[5] J. Villén, E. Borràs, W.M.M. Schaaper, R.H. Meloen, M. Dávila, E. Domingo, E. Giralt, D. Andreu, ChemBioChem 3 (2002) 175–182.
[6] Y. Nishida, T. Tsurumi, K. Sasaki, K. Watanabe, H. Dohi, K. Kobayashi, Org. Lett. 5 (2003) 3775–3778.
[7] S. Fournel, S. Wieckowski, W. Sun, N. Trouche, H. Dumortier, A. Bianco, O. Chaloin, M. Habib, J.-C. Peter, P. Schneider, B. Vray, R.E. Toes, R. Offringa, C.J.M. Melief, J. Hoebeke, G. Guichard, Nat. Chem. Biol. 1 (2005) 377–382.
[8] C. Hunke, T. Hirsch, J. Eichler, ChemBioChem 7 (2006) 1258–1264.
[9] K. Marotte, C. Préville, C. Sabin, M. Moumé-Pymbock, A. Imberty, R. Roy, Org. Biomol. Chem. 5 (2007) 2953–2961.
[10] N. Trouche, S. Wieckowski, W. Sun, O. Chaloin, J. Hoebeke, S. Fournel, G. Guichard, J. Am. Chem. Soc. 129 (2007) 13480–13492.
[11] H.M. Maric, V.B. Kasaragod, L. Haugaard-Kedström, T.J. Hausrat, M. Kneussel, H. Schindelin, K. Strømgaard, Angew. Chem. Int. Ed. 54 (2015) 490–494.
[12] D. Spencer, T. Wandless, S. Schreiber, G. Crabtree, Science 262 (1993) 1019–1024.
[13] A. Bach, B.H. Clausen, M. Møller, B. Vestergaard, C.N. Chi, A. Round, P.L. Sørensen, K.B. Nissen, J.S. Kastrup, M. Gajhede, P. Jemth, A.S. Kristensen, P. Lundström, K.L. Lambertsen, K. Strømgaard, Proc. Natl. Acad. Sci. 109 (2012) 3317–3322.
[14] A. Bianco, S. Fournel, S. Wieckowski, J. Hoebeke, G. Guichard, Org. Biomol. Chem. 4 (2006) 1461–1463.
[15] H.-S. Moon, E.M. Jacobson, S.M. Khersonsky, M.R. Luzung, D.P. Walsh, W. Xiong, J.W. Lee, P.B. Parikh, J.C. Lam, T.-W. Kang, G.R. Rosania, A.F. Schier, Y.-T. Chang, J. Am. Chem. Soc. 124 (2002) 11608–11609.
[16] J.H. Lee, A.M. Meyer, H.-S. Lim, Chem. Commun. 46 (2010) 8615–8617.
[17] M. Oh, J.H. Lee, W. Wang, H.S. Lee, W.S. Lee, C. Burlak, W. Im, Q.Q. Hoang, H.-S. Lim, Proc. Natl. Acad. Sci. 111 (2014) 11007–11012.
[18] M. Oh, J.H. Lee, H. Moon, Y.-J. Hyun, H.-S. Lim, Angew. Chem. Int. Ed. 55 (2016) 602–606.
[19] D. Scharn, H. Wenschuh, U. Reineke, J. Schneider-Mergener, L. Germeroth, J. Comb. Chem. 2 (2000) 361–369.
[20] J.T. Bork, J.W. Lee, S.M. Khersonsky, H.-S. Moon, Y.-T. Chang, Org. Lett. 5 (2003) 117–120.
[21] M.A. Clark, R.A. Acharya, C.C. Arico-Muendel, S.L. Belyanskaya, D.R. Benjamin, N.R. Carlson, P.A. Centrella, C.H. Chiu, S.P. Creaser, J.W. Cuozzo, C.P. Davie, Y. Ding, G.J. Franklin, K.D. Franzen, M.L. Gefter, S.P. Hale, N.J. Hansen, D.I. Israel, J. Jiang, M.J. Kavarana, M.S. Kelley, C.S. Kollmann, F. Li, K. Lind, S. Mataruse, P.F. Medeiros, J.A. Messer, P. Myers, H. O'Keefe, M.C. Oliff, C.E. Rise, A.L. Satz, S.R. Skinner, J.L. Svendsen, L. Tang, K. van Vloten, R.W. Wagner, G. Yao, B. Zhao, B.A. Morgan, Nat. Chem. Biol. 5 (2009) 647–654.
[22] R. Banerjee, N.J. Pace, D.R. Brown, E. Weerapana, J. Am. Chem. Soc. 135 (2013) 2497–2500.
[23] H.A.H. Elshemy, E.K.A. Abdelall, A.A. Azouz, A. Moawad, W.A.M. Ali, N.M. Safwat, Eur. J. Med. Chem. 127 (2017) 10–21.
[24] D. Scharn, L. Germeroth, J. Schneider-Mergener, H. Wenschuh, J. Org. Chem. 66 (2001) 507–513.
[25] J.H. Lee, H.-S. Kim, H.-S. Lim, Org. Lett. 13 (2011) 5012–5015.
[26] H. Hermeking, Nat. Rev. Cancer 3 (2003) 931–943.
[27] S. Sun, E.W.P. Wong, M.W.M. Li, W.M. Lee, C.Y. Cheng, J. Endocrinol. 202 (2009) 327–336.
[28] Y. Liu, H. Liu, B. Han, J.-T. Zhang, Cancer Res. 66 (2006) 3248–3255.
[29] C. Ottmann, Biorg. Med. Chem. 21 (2013) 4058–4062.
[30] H. Wu, J. Ge, S.Q. Yao, Angew. Chem. Int. Ed. 49 (2010) 6528–6532.
[31] V. Corradi, M. Mancini, F. Manetti, S. Petta, M.A. Santucci, M. Botta, Bioorg. Med. Chem. Lett. 20 (2010) 6133–6137.
[32] P. Parvatkar, N. Kato, M. Uesugi, S.-I. Sato, J. Ohkanda, J. Am. Chem. Soc. 137 (2015) 15624–15627.
[33] L.-G. Milroy, M. Bartel, M.A. Henen, S. Leysen, J.M.C. Adriaans, L. Brunsveld, I. Landrieu, C. Ottmann, Angew. Chem. Int. Ed. 54 (2015) 15720–15724.
[34] G. Hu, Z. Cao, S. Xu, W. Wang, J. Wang, Sci. Rep. 5 (2015) 16481–16493.
[35] L.M. Stevers, E. Sijbesma, M. Botta, C. MacKintosh, T. Obsil, I. Landrieu, Y. Cau, A.J. Wilson, A. Karawajczyk, J. Eickhoff, J. Davis, M. Hann, G. O'Mahony, R.G. Doveston, L. Brunsveld, C. Ottmann, J. Med. Chem. 61 (2018) 3755–3778.
[36] M.B. Yaffe, K. Rittinger, S. Volinia, P.R. Caron, A. Aitken, H. Leffers, S.J. Gamblin, S.J. Smerdon, L.C. Cantley, Cell 91 (1997) 961–971.
[37] P.J. de Vink, J.M. Briels, T. Schrader, L.-G. Milroy, L. Brunsveld, C. Ottmann, Angew. Chem. Int. Ed. 56 (2017) 8998–9002.
[38] E. Yilmaz, D. Bier, X. Guillory, J. Briels, Y.B. Ruiz-Blanco, E. Sanchez-Garcia, C. Ottmann, M. Kaiser, Chem. Eur. J. 24 (2018) 13807–13814.
[39] S.C. Masters, H. Fu, J. Biol. Chem. 276 (2001) 45193–45200.
[40] C.H.S. Lu, H. Sun, F.B. Abu Bakar, M. Uttamchandani, W. Zhou, Y.-C. Liou, S.Q. Yao, Angew. Chem. 120 (2008) 7548–7551.
[41] K. Vanommeslaeghe, E. Hatcher, C. Acharya, S. Kundu, S. Zhong, J. Shim, E. Darian, O. Guvench, P. Lopes, I. Vorobyov, A.D. Mackerell Jr., J. Comput. Chem. 31 (2010) 671–690.